Analysis of Geomaterials using Frequency Modulated Continuous Wave Radar in the X-band

Jamie Blanche, Dr. David Flynn, Dr. Helen Lewis, Prof. Gary Couples
Heriot Watt University
Edinburgh, United Kingdom
jrb31@hw.ac.uk, D.Flynn@hw.ac.uk, Helen.Lewis@pet.hw.ac.uk, Gary.Couples@pet.hw.ac.uk

Prof. Rebecca Cheung
Scottish Microelectronics Centre
University of Edinburgh
Edinburgh, United Kingdom
r.cheung@ed.ac.uk

***Abstract*— In this paper we explore the suitability of Frequency Modulated Continuous Wave sensing for geomaterial property classification. Seminal results derived from analysis of return signal amplitude and phase over a frequency bandwidth of 9.25 – 10.75 GHz are presented. Due to advances in microwave electronics, our evaluation explores the concept of a novel desktop analysis system for real-time monitoring of geomaterial properties. A range of geomaterial samples are analysed including, Darney, Locharbriggs and Red St. Bees Sandstones. Ambient environment ground truth measurements are compared to samples imbibed with deionised (DI) water. Results indicate that each geomaterial sample can be clearly identified, with the Darney Sandstone exhibiting the clearest response to fluid ingress, with a phase shift relative to a "dry" sample of 126° for DI water. The results of these preliminary experiments support the sensitivity of the FMCW sensing modality to variances in geomaterial properties.**

Keywords—Condition monitoring, Microwaves, X-band, Non-destructive testing, Petroleum industry, FMCW radar

I. INTRODUCTION

Reservoir management is used throughout the life cycle of oil and gas fields and is integral to safe and efficient recovery of resources. An essential tool of reservoir management is a mass–fluid flow simulation, within which different production scenarios can be trialled and their practical, economic and environmental consequences investigated. Such simulations are dependent on the arrangement and properties of the *in situ* geomaterials and the responses of those materials to subsurface and production-induced conditions. Geomaterial properties directly influence hydrocarbon recovery factors, as do operational choices. The same concepts apply to sites investigated for carbon storage and also provide a means of mitigating risk when sites are exposed to extreme loading events.

Today, improvements in seismic acquisition and processing technology, in addition to sophisticated wire-line sensors available for use in a wellbore environment, are used to generate useful models of the distribution of the geomaterials in the subsurface. However seismic-based techniques are insufficient to provide data at the sub-centimetre scale, such as the grain-pore structures, and contain significant uncertainties. Such pore-scale knowledge can be used to derive continuum-scale properties that are needed for flow simulations. Non-destructive x-ray and acoustic, and similar tomographic studies [1, 2], can also provide distributions of material density or acoustic velocity. The purpose of this work is to extend the range of tool types and measurements obtained over this size range via the novel use of advanced radar electronics.

First available in the 1970's, FMCW deployment in civilian radar systems was impractical due to power demands and excessive size. The technology found use in high end vehicles and research applications but was not practically deployable in portable systems until the late 1990's [3]. The chosen frequency band, the required return signal properties and measurands, thus, the antenna dimensions, define the size of the electronics and associated hardware. Modern advances in electronic miniaturisation and power economy have led to the deployment of FMCW radar systems into sensitive and harsh environments as a matter of routine. Analogous to advances in desktop computing systems, corresponding to a reduction in unit size, power consumption and cost, this advance in microwave electronic efficiency is expected to continue as demand for active measurement is perpetuated by the development of the Internet of Things (IoT) and deployable smart systems.

Following an investigation into candidate non-destructive inspection/evaluation (NDI/NDE) technologies, we explore the application of frequency modulated continuous wave (FMCW) sensing for the characterisation of geomaterial pore spaces and the determination of fluid-phase occupancies. Microwaves within the X-band represent a

non-destructive and non-contact means of inspection, with the potential to reveal intrinsic properties of the geomaterial target. FMCW technology has seen wide application within the industrial and automotive sectors for distance and velocity sensing [4, 5]. Millimetre wave FMCW radar has been successfully applied in defence roles, such as concealed weapon and explosive detection, surveillance and perimeter security and roadside device detection [6]. FMCW radar has also seen use in medical imaging and research, with a proven capability to detect displacement at the sub-micron level for respiration and heartbeat monitoring [7-9]. Investigations into the application of X-band FMCW as a stratigraphic tool for research into snow and ice dynamics have also provided data relating to geometrical layering, density, water equivalence, total snow height and moisture content [10-12]. In other applications, recent work has focused upon the use of FMCW to locate corrosion under insulation (CUI) in pipeline assets [13, 14]. However, to date, there has been little or no research into the application of this technology for geomaterial analysis, and the authors believe that the results reported within this paper represent the potential for a new instrument for dynamic and quasi-static geomaterial analysis and a first for FMCW radar electronics in this role. These multi-disciplinary applications indicate that there is potential for FMCW radar to return significant information about the constituent materials and their arrangements within a geomaterial sample: grain, cement, matrix and fluid-filled pore contents, via analysis of the dielectric response to incident microwave radiation, delivering a step-change in geomaterial characterisation. An assessment of FMCW signal return in the K-band was conducted on eight geomaterial samples in [15] with the results indicating clear differences in relative permittivities between these geomaterials. Informed by this previous research, the current research schedule was adapted to evaluate five sandstones of approximately uniform bulk mineralogy.

Section II will outline the theory of FMCW sensing. Section III will address the application of FMCW to geomaterials. Section III/A will discuss dielectric theory, section III/B will examine the complex refractive index method (CRIM) and section III/C will discuss reflective phase angle. Section IV will describe sample preparation and experimental procedure followed by section V, which will display data acquired for a partially saturated (50 – 60%) sandstone layer contained within a dry stack of sandstones, at ambient laboratory conditions, and will discuss the observed results. Section VI will conclude, with suggestions for further work contained in section VII.

II. Frequency Modulated Continuous Wave Radar Theory

FMCW represents a continuous wave instead of the more commonly used pulsed wave radar. Frequency modulation gives a frequency shift over time to create a saw-tooth or triangular frequency output. A difference in frequency between the transmitted and received signals is determined by mixing output and input waveforms to give a new, low frequency signal, which can be analysed to calculate the distance and velocity of an object. The difference in frequency observed between received and output signals is calculated and transmitted to a data logger as an Intermediate Frequency (IF) signal of frequency Δf. An overview of the determination of the IF signal of frequency Δf is as follows :

$$f_{\mathrm{RFOUT}} = f_{\mathrm{RF0}} + k_{\mathrm{f}} * t,\ where\ 0 \leq t \leq T \tag{1}$$

f_{RFO} is the starting frequency, T is the frequency sweep and k_f is the sweep rate.

$$k_{\mathrm{f}} = \frac{BW}{T} \tag{2}$$

where BW is the frequency bandwidth for the sweep and with the two way time (TWT) of the emitted signal calculated as:

$$\Delta t = 2\frac{d}{c} \tag{3}$$

where d is the distance between the antenna and the reflecting target and c is the speed of light in the medium of propagation. Therefore, due to the observed delay in return signal, the return frequency compared to the emitted frequency will be:

$$f_{\mathrm{RF\ received}} = f_{\mathrm{RF0}} + k_{\mathrm{f}} * (t - \Delta t),\ \Delta t \leq t \leq T + \Delta t \tag{4}$$

The difference in frequency (Δf) between the emitted and received signal is therefore:

$$\Delta f = k_{\mathrm{f}} * (-\Delta t) \tag{5}$$

It is this difference in frequency that is output from the detector as data. The negative time of flight can be taken as a magnitude, allowing for the expression:

$$\Delta f = \frac{BW}{T} * 2\frac{d}{c} \tag{6}$$

Due to the relationship expressed in (6), z-axis distance between the sensor and geomaterial sample is kept constant. Thereby, any signal variation can be attributed to the geomaterial intrinsic properties. The properties of the material that influence the signal parameters are outlined in the following section.

III. Application of FMCW to Geomaterial Samples

In this section we examine the primary return signal parameters. X-band analysis over a sweep in frequency offers key advantages over a pulsed, single frequency method. These are: improved signal to noise characteristics

due to a broader frequency range, a lower intermediate frequency (IF), relative immunity to harsh ambient conditions, a lack of requirement to make physical contact with the material under investigation and a lower signal attenuation, compared to K-band FMCW, due to a longer wavelength.

Dielectric relaxation processes govern wave attenuation and dispersion within dielectric materials, as defined by the relative permittivity, ε^*. These relaxation processes are influenced by the frequency of the incident radiation, where constituent materials throughout the component scale range damp localised oscillations. The multiple relaxation modes acting simultaneously within an irradiated material generate significant non-linearity and can complicate data analysis. However, the information provided by this complex returned signal allow for feature extraction relevant to dielectric material properties. In geomaterials, the relative permittivity is affected by the many factors, including; pore fluid types and phase, value of porosity, the abundance of high permittivity mineral inclusions and grain long axis orientation, all defined by the dielectric relaxation [16]. It is the dielectric response of the geomaterial that has informed the selection of the X-band for this work. Previous experimentation conducted by this group has focused on the use of K-band FMCW to generate a signal response specific to the presence of water within a sample [15]. It is well documented that K-band radiation undergoes significant attenuation due to heavy absorption at these frequencies, specifically centred around 22.5 GHz due to radiation absorption by water. This effect has led to the partitioning of the K-band into the Ku and Ka bands (12-18 GHz and 26.5–40 GHz respectively). Within section III/A, we introduce the dielectric theory associated with the intrinsic dielectric constant property of a material. Investigation in the X-band allows for deeper penetration within the sample material due to a reduction in water-induced signal attenuation and dispersion.

A. Dielectric Theory

Equation (7) represents the component form of ε^*, the relative electrical permittivity of a particular medium. ε', represents the observed and real relative permittivity of the material in an idealised form. The complex component, $j\varepsilon''$, denotes the "loss factor" of the material and therefore represents the dispersion of incident radiation due to conduction and relaxation of atomic constituents.

$$\varepsilon^* = \varepsilon' + j\varepsilon'' \tag{7}$$

In many theoretical instances, the complex component of this relationship is ignored, as materials used for dielectric media tend to be poor conductors. However, applications within geomaterial samples could be contrary to this assumption, with many constituent parts of a geomaterial matrix and void spaces offering appreciable conduction, for example, the presence of brines, water and mineral inclusions [17].

Nevertheless, this model operates under the assumption that the component of dielectric loss (the complex term, $j\varepsilon''$, in (7) is much smaller than the real component, representing the reflection data. For an ideal reflector,

$$h(t) = \Sigma_i\, a_i\, \delta(t - \tau_i) \tag{8}$$

B. Complex Refractive Index Method

The complex refractive index method (CRIM) stipulates that the square root of the observed relative permittivity (or dielectric constant) is equal to the product of the fractional porosity of the sample and the square root of the relative permittivity of the pore fluid plus the product of the fractional porosity and the square root of the relative permittivity of the geomaterial matrix taken from unity. Thus, for a simplified, fluid soaked and uniform, porous sandstone,

$$\sqrt{\varepsilon_s} = \left(\phi_f\sqrt{\varepsilon'_f} + \phi_a\sqrt{\varepsilon'_a}\right) + \left(1 - \phi_T\sqrt{\varepsilon'_m}\right) \tag{9}$$

where ε_s is the observed relative permittivity of the investigated sample, ϕ_T is the total measured sample porosity, ϕ_f is the fractional porosity occupied by fluid (determined by mass changes), ϕ_a is the fractional porosity occupied by air, ε'_f is the relative permittivity of a single phase pore fluid, ε'_a is the relative permittivity of the volumetric air content and ε'_m is the relative permittivity of the geomaterial matrix [18]. This is an idealised situation and is unrepresentative of the inclusions to be found in sandstones collected in the field. Therefore (9) should also account for observed material within the samples under investigation. In the case of the Darney, Locharbriggs and Red St. Bees Sandstones, this would include a few pieces of Mica and Feldspar. In principle, detailed knowledge of the geomaterial characteristics would lead to the ability to model the response, which could be compared against measurements. Within section III.C we introduce the relationship between relative permittivity and reflected phase angle.

C. Phase Angle

Using the relation,

$$j\omega\sqrt{\mu_0}\sqrt{\varepsilon' - j\varepsilon''} = \alpha + j\beta \tag{10}$$

where $j\omega$ is the complex component of the angular frequency, α is the attenuation in nepers per metre, β is the phase shift in radians per metre and μ_0 is the vacuum permeability. It can be seen that, for a given attenuation and angular frequency, the real component of the relative permittivity is proportional to the phase shift of an observed return microwave signal, with the expectation that a

complex component of multi-phase pore fluid with a higher phase shift, a factor in (9), will correspond to a higher observed relative permittivity . Section IV will introduce the experimental procedure for the geomaterial analysis and preparation.

IV. Experimental Procedure and Sample Preparation

The apparatus used to create the FMCW signal was a Hewlett-Packard/Keysight 8510 Vector Network Analyser. This device was also used to analyse output source FMCW waveform and was coupled to a Beijing Xibao Electronic Technology Co. standard gain horn antenna (SGH), manufacturer serial number XB-WDB2-18 (NF), capable of radiation output ranging 2–18 GHz and with a nominal gain of 15.74 dBi (at 10 GHz). This antenna was affixed to a static mounting and directed vertically onto the geomaterial samples with the z-axis constant in all measurements at 10 mm.

A. Antenna Characterisation

In order to inform an appropriate geomaterial sample size for this antenna setup, the radiation output was determined as a function of bandwidth sweep. To meet this requirement, three scans were performed using a two-dimensional translation stage coupled to a OEWG standard probe, type WR90, designed to capture microwave radiation intensities in the X-band (8–12 GHz). Using a non-radiative near-field separation distance between the probe and the antenna under test (AUT) of 14 cm, three data sets were acquired representing the limits and median of the 1500 MHz bandwidth sweep, 9.25, 10 and 10.75 GHz respectively with Fig. 1 and 2 showing the radiation pattern for 10 GHz.

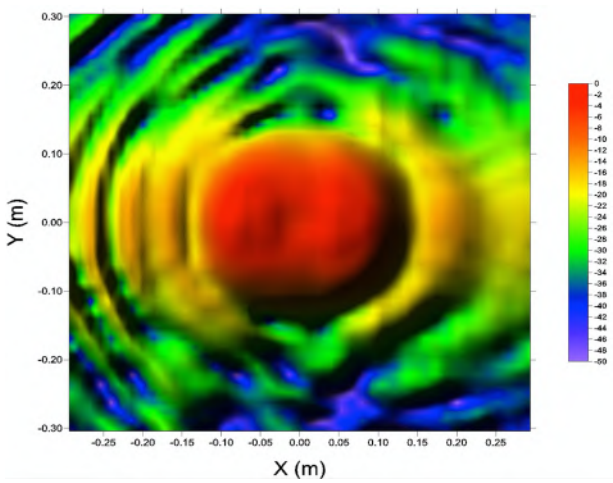

Fig. 1. Radiation pattern for 10 GHz (scale bar in dBm)

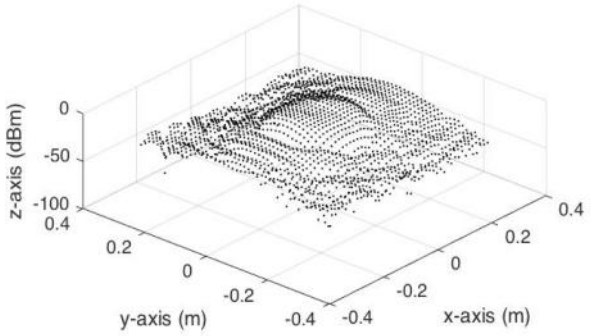

Fig. 2. 3D Radiation pattern for 10 GHz

B. Sample Preparation

Acquired from Stancliffe Stones of Alfreton, three sandstone geomaterial samples (100 mm x 100 mm x 12 mm) of UK origin were tested, with sample size informed by the antenna characterisation. The sample sandstones are: Darney, Locharbriggs and Red St. Bees. These samples were chosen due to their well-documented intrinsic properties and to represent a varying range of geomaterial complexities (e.g. uniformity vs. layering). Each sample was expected to possess approximately uniform bulk mineralogy, but to also contain detectable differences in grain structure, orientation, distribution and porosity.

C. Data Acquisition

Each sample, illustrated in Fig. 3 right, was scanned at ambient laboratory conditions. The samples were heated in a Carbolite oven for 5 hours at 60^{o}C to remove any humidity within the pore spaces and then weighed to acquire the "dry" mass. Each sample was then immersed in deionised water for 250 minutes for the first experimental run and for 168 hours for the second. Once extracted from the saturation fluid and excess fluid removed, the samples were again weighed to obtain "wet" mass measurements and to calculate the degree of saturation. Each sample was then scanned by X-band FMCW to obtain ground truth measurements for both "dry" and "wet" (partially saturated) conditions. The samples were dried in an oven at 60^{o}C for 6 hours to remove the imbibed water, and were observed to return to their "dry" weight. Calculated partial saturation values for deionised water are given in Table 1. An experiment was setup to measure the effect of a partially saturated layer of sandstone as a function of proximity to the sensor head. This required the stacking of the five sandstone sections and cycling a layer of partially saturated geomaterial up the stacked arrangement of rocks, from position 5 through 1, as illustrated in Fig. 3. Each sandstone sample was 12 mm thick, giving a total stack depth of 60 mm. Section V contains results and observations of the acquired data.

Fig. 3. Stacked sandstone arrangement for saturated layer proximity test (numbered positions shown)

TABLE 1. PARTIAL SATURATION VALUES FOR SANDSTONE IN DEIONISED WATER

Soak time = 250 minutes	
Sample	***Porosity volume occupied by DI water (%)***
Locharbriggs	55.07
Red St. Bees	58.43
Darney	52.27
Soak Time = 168 hours	
Sample	***Porosity volume occupied by DI water (%)***
Locharbriggs	59.52
Red St. Bees	67.70
Darney	61.01

V. RESULTS AND DISCUSSION

Observations have been taken at a fixed near-field horn distance of 10 mm with Fourier transforms providing frequency domain phase-shift data. It can be seen from Fig. 6 and 7 that the presence of a partially saturated layer of sandstone, in this case, Locharbriggs Sandstone, within a predominantly dry sandstone stack will result in a significant difference to the return of a X-band FMCW signal. Fig. 4 and 5 illustrate the effect on dry sample signal variance for the experiment described in Section IV. This data provides verification that, for dry samples only, the return signal contains small variations for the Locharbriggs sandstone as a function of proximity to the X-band sensor head/antenna. The same experiment repeated for a partially saturated Locharbriggs sandstone sample exhibits a significantly greater signal variance as a function of proximity to the sensor head. An analysis of this data shows that the return signal phase variance as a function of proximity of the partially saturated sample to the sensor head is affected significantly, with results shown in Table 2 verifying the expected progression of phase shift as a function of the change in relative permittivity due to a shift in the ratio of imbibed deionised water and air content within the sample pore spaces.

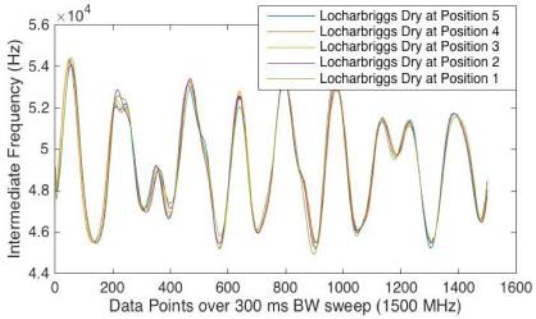

Fig. 4. Dry stacked intermediate frequency output (time domain)

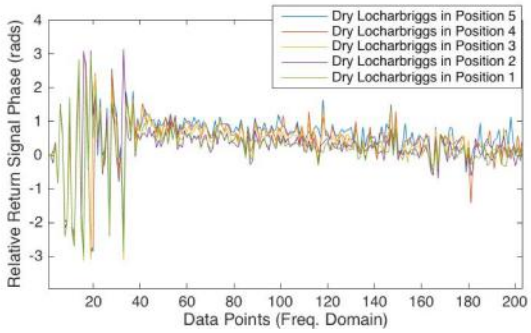

Fig. 5. Dry stacked phase correlation in frequency domain

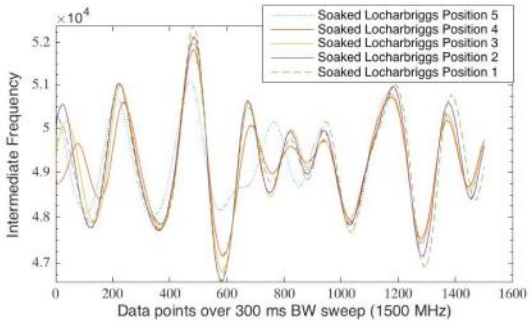

Fig. 6. Partially saturated stacked intermediate frequency output in time domain

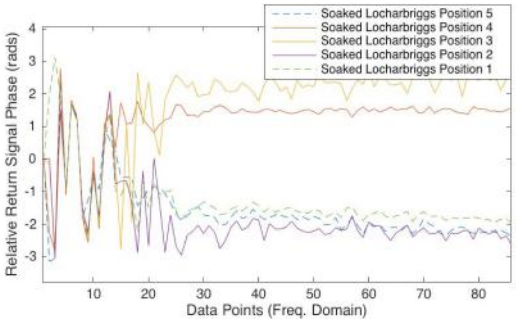

Fig. 7. Partially saturated stacked phase with phase differences clearly discernable as a function of proximity to sensor head.

TABLE 2. FIRST INTERFACIAL PHASE VALUES OBSERVED FOR SANDSTONE SAMPLES AFTER DEIONISED WATER SOAKING (FOR 4 HOURS AND 168 HOURS)

Sample	*Saturation*	*Rads*	*θ ·*	*Δθ ·*
Darney	*Dry*	*0.11*	*6.11*	*0.00*
	Wet (4hr)	*2.31*	*132.60*	*126.49*
	Wet (168hr)	*1.60*	*91.88*	*85.77*
Locharbriggs	*Dry*	*3.09*	*177.20*	*0.00*
	Wet (4hr)	*2.83*	*162.18*	*-15.02*
	Wet (168hr)	*2.35*	*134.48*	*-42.72*
Red St. Bees	*Dry*	*3.10*	*177.53*	*0.00*
	Wet (4hr)	*2.74*	*156.69*	*-20.84*
	Wet (168hr)	*2.44*	*139.86*	*-37.67*

VI. CONCLUSION

In this work, we outlined a novel instrument that capitalises on high performance electronics, in addition to a unique application of the FMCW sensing modality. This highly multidisciplinary work has targeted the interfaces between electronics, sensing and materials and has demonstrated that the FMCW method provides significant differences in return signal amplitude and phase that can be observed to correspond with differences in geomaterial specimens. It can also be observed that mineralogical characteristics of the specimens tested have a plausible relationship with the return signal in terms of amplitude and phase, with unique signatures acquired for each geomaterial specimen.

VII. FURTHER WORK

Future work will examine in greater detail the interaction of electromagnetic waves with varying intrinsic structures that define geomaterials through experimental and simulated analysis. Involving the fabrication of geomaterial analogues and multi-physics modelling techniques, in addition to the analysis of sandstone and limestone samples via X-ray and neutron beam radiation to corroborate dielectric responses in the X- and K-bands. This research will inform an optimal design process, influencing frequency bandwidth, horn antenna design and signal analysis methods in relation to monitoring lithological boundaries, lamination and multi-phase pore content dynamics.

REFERENCES

[1] E.-M. Charalampidou, S. A. Hall, S. Stanchits, G. Viggiani, and H. Lewis, "Shear-enhanced compaction band identification at the laboratory scale using acoustic and full-field methods," *International Journal of Rock Mechanics and Mining Sciences,* vol. 67, pp. 240-252, 2014.

[2] E.-M. Charalampidou, S. A. Hall, S. Stanchits, H. Lewis, and G. Viggiani, "Characterization of shear and compaction bands in a porous sandstone deformed under triaxial compression," *Tectonophysics,* vol. 503, pp. 8-17, 2011.

[3] J. r. Hasch, E. Topak, R. Schnabel, T. Zwick, R. Weigel, and C. Waldschmidt, "Millimeter-Wave Technology for Automotive Radar Sensors in the 77 GHz Frequency Band," *IEEE Transactions on Microwave Theory and Techniques,* vol. 60, pp. 845-860, 2012.

[4] P. Kaminski, K. Staszek, K. Wincza, and S. Gruszczynski, "K-band FMCW Radar Module with Interferometic Capability for Industrial Applications," presented at the 15th International Radar Symposium (IRS), 2014.

[5] R. Yadav, P. K. Dahiya, and R. Mishra, "A High Performance 76.5 GHz FMCW RADAR for Advanced Driving Assistance System," in *3rd International Conference on Signal Processing and Integrated Networks (SPIN)*, Noida, India, 2016, pp. 383-388.

[6] P. D. L. Beasley, "Advances in Millimetre Wave FMCW Radar," in *MRRS-2008 Symposium Proceedings*, Kiev, Ukraine, 2008.

[7] G. Vinci, S. Lindner, F. Barbon, M. Hofmann, D. Fischer, D. Kissinger*, et al.*, "24 GHz Six-Port Medical Radar for Contactless Respiration Detection and Heartbeat Monitoring," in *9th European Radar Conference*, Amsterdam, The Netherlands, 2012.

[8] O. Aardal, Y. Paichard, S. Brovoll, T. Berger, T. S. Lande, and S. E. Hamran, "Physical working principles of medical radar," *IEEE Trans Biomed Eng,* vol. 60, pp. 1142-9, Apr 2013.

[9] C. Li, V. M. Lubecke, O. Boric-Lubecke, and J. Lin, "A Review on Recent Advances in Doppler Radar Sensors for Noncontact Healthcare Monitoring," *IEEE Transactions on Microwave Theory and Techniques,* vol. 61, pp. 2046-2060, 2013.

[10] H. Gubler and M. Hiller, "The use of microwave FMCW radar in snow and avalanche research," *Cold Regions Science and Technology,* vol. 9, pp. 109 - 119, 31st July 1984 1984.

[11] J. Holmgren, M. Sturm, N. E. Yankielun, and G. Koh, "Extensive measurements of snow depth using FM-CW radar," *Cold Regions Science and Technology,* vol. 27, pp. 17 - 30, 1998.

[12] H.-P. Marshall and G. Koh, "FMCW radars for snow research," *Cold Regions Science and Technology,* vol. 52, pp. 118-131, 2008.

[13] R. E. Jones, F. Simonetti, M. J. S. Lowe, and I. P. Bradley, "Use of Microwaves for the Detection of Water as a Cause of Corrosion Under Insulation," *Journal of Nondestructive Evaluation,* vol. 31, pp. 65-76, 2011.

[14] D. S. Herd, "Microwave Based Monitoring System for Corrosion Under Insulation," Doctor of Philosophy, Institute of Signals, Sensors and Systems, School of Engineering and Physical Sciences, Heriot-Watt University, Heriot-Watt University, 2016.

[15] J. Blanche, D. Flynn, H. Lewis, G. Couples, and R. Cheung, "Analysis of Geomaterials using Frequency Modulated Continuous Waves," presented at the Thirteenth International Conference on Condition Monitoring and Machinery Failure Prevention Technologies, Paris, 2016.

[16] J. H. Bradford and H. Marshall, "Estimating complex dielectric permittivity of soils from spectral ratio analysis of swept frequency (FMCW) ground-penetrating radar data," in *American Geophysical Union, Fall Meeting 2010*, 2010.

[17] J. H. Schön, *Physical Properties of Rocks: A Workbook* vol. 8. The Boulevard, Langford Lane, Kidlington, Oxford, OX5 1GB, UK: Elsevier, 2011.

[18] R. P. Wharton, G. A. Hazén, R. N. Rau, and D. L. Best, "Electromagnetic Propagation Logging: Advances in Technique and Interpretation," presented at the SPE Annual Technical Conference and Exhibition, 1980.

Sponsored by the Energy Technology Partnership (ETP) and Maersk.